Progress In Electromagnetics Research Letters, Vol. 69, 127–132, 2017

A Compact Ultra-Wideband Bandpass Filter with Sharp Roll-off Based on CPW-to-Microstrip Coupling Structure

Qiong Wang[1], Chunhui Shi[3], Xinlin Xia[2, *], Zhong Wang[3], and Yu Huang[1]

Abstract—In this paper, a compact ultra-wideband bandpass filter using a back to back Coplanar Waveguide (CPW)-to-microstrip transition structure is proposed. Compared with traditional ultra-wideband bandpass filters using hybrid structures, the proposed filter has a sharper selectivity because of two transmission zeros located at the lower and upper edges of the passband, respectively, generated by a modified T-shaped stub. Moreover, to further improve its out-of-band performance open stubs are introduced to produce extra transmission zeros at high frequency. A prototype of the proposed filter is fabricated and measured. The results show that the proposed filter achieves a bandwidth of 133% from 2.4 to 11.9 GHz, and the selectivity (skirt factor) is optimized from 50% to 92% compared to a former ultra-wideband (UWB) bandpass filter (BPF) with a similar structure. Besides, the proposed filter can offer some other advantages such as good return loss, low insertion loss, stable group delay, and compact size ($16 \times 7.55\,\mathrm{mm}^2$). This filter can be a good candidate for UWB applications.

1. INTRODUCTION

Since the US Federal Communication Commission (FCC) authorized the ultra-wideband (UWB) spectrum (3.1 to 10.6 GHz) for commercial use in 2002 [1], the UWB bandpass filter, as a key passive component in a UWB system, has received much interest. In recent years, several methods and structures have been proposed to implement UWB bandpass filter (BPF) with compact size, sharp roll-off, low insertion loss and wide bandwidth [2–18]. Among the reported UWB BPFs, the interdigital coupled-line, which can create a UWB bandpass response and the multi-mode resonators (MMR) are the most widely used structures [2–7]. In [2, 3], UWB bandpass filters with sharp selectivity were realized using MMR. Similarly, the stepped-impedance stub-loaded resonators were often applied in UWB BPF to improve the out-of-band performances in [4, 5]. The upper stopband performances were improved by introducing tri-section stepped-impedance resonators (TSSIR) in [6, 7]. However, the selectivity is bad because there was no transmission zero in the low frequency band not including 0 GHz. At the same time, several other UWB BPFs have been reported based on the hybrid structures. For example, CPW-to-microstrip transitions structures [8, 10] and microstrip-to-CPW transition structures [11, 12] have been used to design UWB BPFs. In these filters, their main structures are microstrip-CPW or CPW-microstrip transition. Even though the transition structures have bandpass characteristic, their stopband characteristics are dissatisfactory. In [13], a novel UWB BPF using slow-wave half-mode substrate-integrated waveguide (SW-HMSIW) with a notch band created by an L-type resonator was presented. Moreover, some novel methods and structures such as the transversal signal-interaction [14, 15], defected microstrip structures (DMS) [16, 17] and defected ground structures (DGS) [18] have been proposed in the last few years. However, the use of DMS and

Received 17 June 2017, Accepted 4 August 2017, Scheduled 14 August 2017
* Corresponding author: Xinlin Xia (xxl0702@sina.cn).
[1] The Engineering Technical College of Chengdu University of Technology, Leshan 614000, China. [2] Microsystem and Terahertz Research Center, China Academy of Engineering Physics, Chengdu 610000, China. [3] Ji Lin Information and TelecommunicatiWon Company of Ji Lin Electric Power Company, Changchun, China.

DGS etched in the microstrip and ground plane, respectively, might destroy the signal integrity for packaging.

In this paper, a UWB bandpass filter with good in-band and out-of-band performances implemented based on hybrid CPW and microstrip structures is proposed as shown in Fig. 1. The basic structure is a back-to-back microstrip–CPW transition structure reported in [8], which can create a UWB bandpass response. In this work, to obtain a UWB BPF with good out-of-band performances, some other structures are used. At first, in order to improve its selectivity, two transmission zeros are introduced by loading a modified T-shaped stub. Moreover, open stubs are applied to further improve the performance of the upper-stopband. In comparison with some traditional UWB BPFs based on hybrid CPW and microstrip structures, the proposed UWB BPF has wider bandpass width and sharper selectivity. Finally, a filter prototype is designed, fabricated and measured to verify its performance, and the test results exhibit a good consistency with the simulated ones.

2. FILTER ANALYSIS AND DESIGN

The basic architecture of the proposed filter is shown in Fig. 1. The opposite sides of the substrate are used as CPW and microstrip line separately. The transition between CPW and microstrip line is based on an electromagnetic coupling mechanism that could be equivalent to a J inverter as shown in Fig. 2. The microstrip MMR consists of step-impedance microstrip lines (TL_5 and TL_4), a T-shaped stub and open stubs even though the transition structure of CPW to microstrip has a UWB bandpass characteristic, and it cannot be used directly in UWB systems due to its bad selectivity. In this work, to obtain a UWB BPF with sharp selectivity, a modified T-shaped stub is loaded at the centre of the microstrip to produce two transmission zeros located at the lower and upper edges of the passband. Moreover, in order to further improve its upper stopband performances, a sector stub and open stubs are used to implement two extra transmission zeros located at high frequencies.

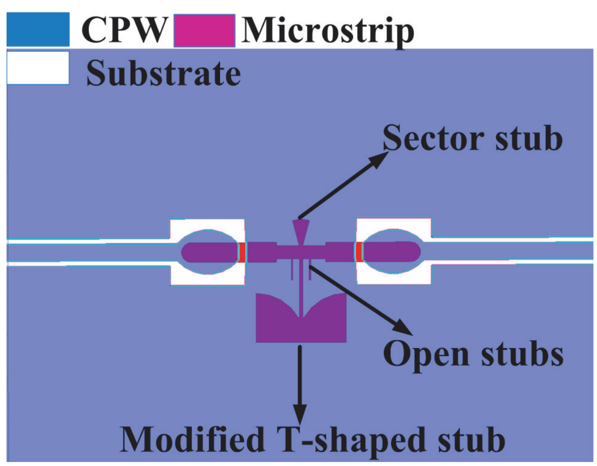

Figure 1. Configuration of the proposed UWB BPF.

As for the modified T-shaped stub, the equivalent transmission lines mode is shown in Fig. 2. And its input impedance (Z_{in1}) is shown in Eq. (1).

$$Z_{in1} = Z_2 \frac{-0.5jZ_1 \cot\theta_1 + jZ_2 \tan\theta_2}{Z_2 + 0.5Z_1 \cot\theta_1 \tan\theta_2} \tag{1}$$

The condition of generating transmission zero Z_{in1} can be expressed by Eq. (2). With the hypothesis of $\theta_1 = \theta_2 = \theta$, its solution can be shown as Eqs. (3)–(4).

$$\tan\theta_1 \tan\theta_2 = \frac{Z_1}{2Z_2} \tag{2}$$

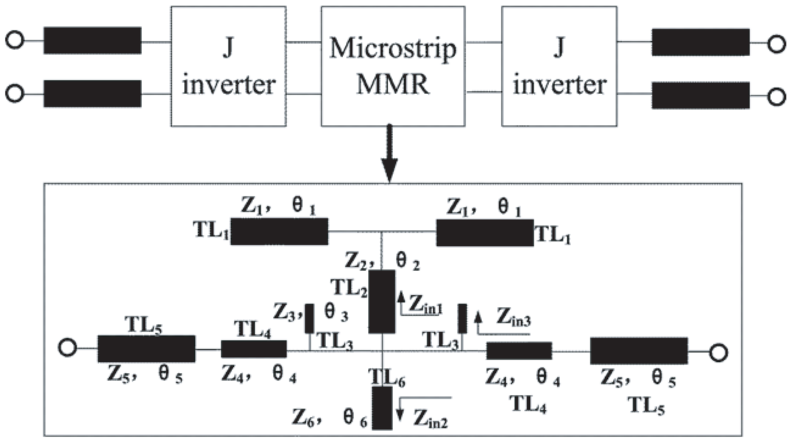

Figure 2. Equivalent J-inverter network of the proposed filter.

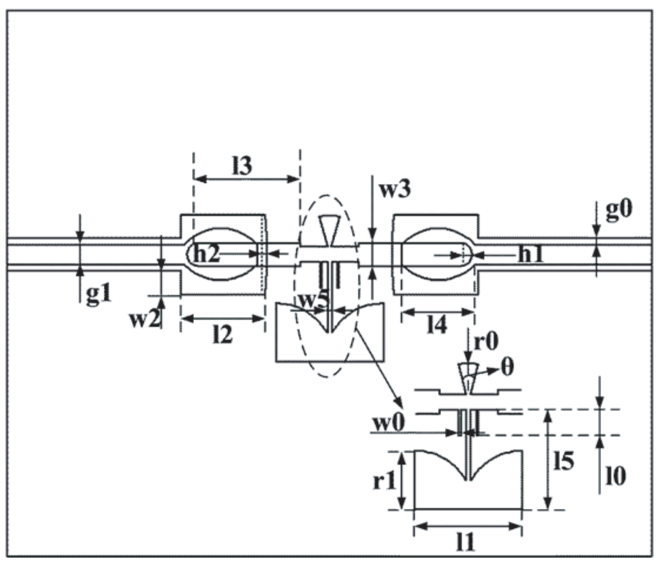

Figure 3. Dimensions of the proposed filter.

$$\theta_1 = \arctan\left(\sqrt{\frac{Z_1}{2Z_2}}\right) \tag{3}$$

$$\theta_2 = \pi - \arctan\left(\sqrt{\frac{Z_1}{2Z_2}}\right) \tag{4}$$

As for the sector stub with a characteristic impedance of Z_6 and open stubs with characteristic impedance of Z_3, the input impedances Z_{in2} and Z_{in3} are shown in Eqs. (5) and (6), respectively.

$$Z_{in2} = -jZ_6 \cot\theta_6 \tag{5}$$

$$Z_{in3} = -jZ_3 \cot\theta_3 \tag{6}$$

Similarly, under the condition of $Z_{in2} = Z_{in3} = 0$, two transmission zeros are generated by the sector and open stubs when $\theta_3 = \theta_6 = \pi/2$.

Finally, the proposed UWB BPF is designed and fabricated for verification. The substrate used in this work is Roger's RO6010, which has a relative permittivity of 10.2 and thickness of 0.635 mm. A photograph of the fabricated filter is shown in Fig. 4.

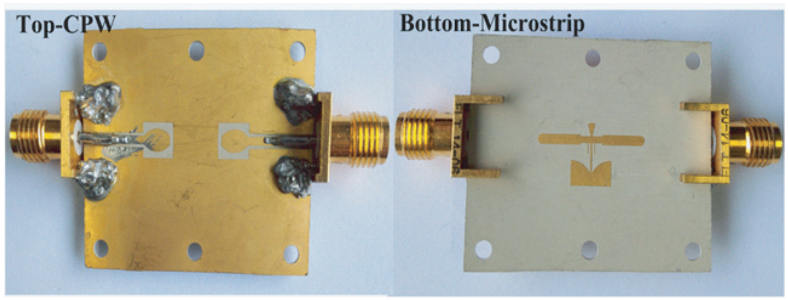

Figure 4. Photograph of the fabricated UWB BPF.

3. EXPERIMENTAL RESULTS

The final dimensions of the fabricated UWB BPF optimized by Ansoft HFSS 13 are (see Fig. 3): $g0 = 0.35\,\text{mm}$, $g1 = 1\,\text{mm}$, $w2 = 1.2\,\text{mm}$, $l2 = 4.6\,\text{mm}$, $h2 = 0.5\,\text{mm}$, $l3 = 5.2\,\text{mm}$, $w5 = 0.22\,\text{mm}$, $w3 = 1.2\,\text{mm}$, $\theta = 30^\circ$, $r0 = 1.6\,\text{mm}$, $w0 = 0.1\,\text{mm}$, $l0 = 1.3\,\text{mm}$, $l5 = 3.75\,\text{mm}$, $h1 = 0.6\,\text{mm}$, $r1 = 3\,\text{mm}$, $l1 = 5.5\,\text{mm}$. To verify our design, the fabricated UWB BPF is measured by an Agilent vector network analyzer E8363B. The measured and EM simulated S-parameters of the proposed UWB BPF are shown in Fig. 5(a). Clearly, a good agreement between the experiment and simulation results is found. The tiny frequency shift is mainly caused by the fabrication and assembly errors. The measured results show that the proposed filter achieves a 3-dB fractional bandwidth of 133% (2.4–11.9 GHz), and the return loss is better than 12 dB from 2.6 to 117 GHz. The measured insertion loss is found less than 0.65 dB within the whole UWB (3.1–10.6 GHz), with a minimum value of 0.44 dB in the vicinity of the central frequency. Moreover, this filter exhibits sharp skirt characteristics. The lower and upper skirt selectivities are 116.3 dB/GHz and 67.5 dB/GHz, respectively, and the selectivity factor (BW|3 dB/BW|30 dB) is 0.9. The simulated and measured group delays for this filter are shown in Fig. 5(b). The group delay is under 0.6 ns in the frequency range of 3 to 11 GHz, and the variation is less than 0.1 ns over the whole UWB passband.

Table 1 summarizes the performance of the proposed filter along with previously published works for comparison. As can be seen, the proposed UWB BPF has sharper selectivity than those previously reported filters. A wider passband width is obtained. Compared to the filter with wide passband

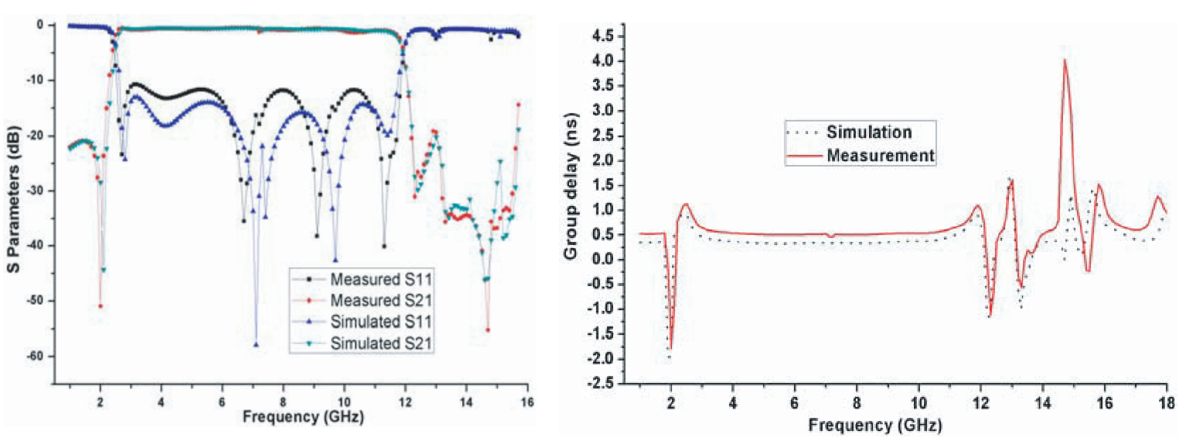

(a) (b)

Figure 5. Simulated and measured results of the fabricated UWB BPF. (a) S parameters, (b) group delay.

Table 1. Comparison with published UWB BPF.

Ref.	Main Structures	BW (%)	RL (dB)	Fc (GHz)	$S.F = \frac{BW\|_{3\,\text{dB}}}{BW\|_{30\,\text{dB}}}$	Size ($\lambda_0 \times \lambda_0$)
[2]	MMR	117	> 10	17.1	0.92	0.51×0.31
[4]	MMR	115	> 10	17.6	0.86	0.38×0.31
[5]	MMR	114	> 10	16.1	0.78	0.73×0.35
[6]	TSSIR	118	> 11	15.4	0.65	1.65×0.41
[7]	TSSIR	119	> 10	30.6	0.6	0.43×0.11
[8]	CPW-to-Microstrip	95	> 11	16	0.5	0.34×0.11
[9]	CPW-to-Microstrip	116	> 15	14	0.5	0.81×0.72
[10]	CPW-to-Microstrip	133	> 15	18	0.83	0.25×0.30
[11]	Microstrip-to-CPW	119	> 16	12	0.77	0.34×0.22
[12]	Microstrip-to-CPW	116	> 14	12.4	0.8	0.33×0.17
[13]	SW-HMSIW	113	> 15	NG	NG	0.60×0.40
[14]	Folded SIR	123	> 12	16.2	0.85	0.54×0.10
[15]	transmission lines	98	> 12	11	0.8	0.69×0.34
[16]	DMS	110	> 10	12	0.77	0.39×0.59
[17]	DMS	129	> 14	18	0.7	0.34×0.08
[18]	DGS	111	> 20	20	0.62	0.25×0.38
This Work	CPW-to-Microstrip + MMR	133	> 12	15.8	0.92	0.36×0.17

S.F.: selectivity factor of the passband; BW: bandpass width; $\Delta f|3\,\text{dB}$, $\Delta f|30\,\text{dB}$: 3 dB bandwidth and 30 dB bandwidth of the passband; Fc: the upper-stopband frequency with 20 dB attenuation level; λ_0: the wavelength at 6.85 GHz NG: Not Given.

using the hybrid CPW and microstrip structures [10], the sharp selectivity is raised from 83% to 92%, and almost 18.4% circuit size reduction is achieved. The proposed filter has almost the same filtering performance as the one using interdigital coupled-line and MMR in [2], but the proposed UWB filter has a wider bandpass width with a size reduction of 61.54%, compared with the one in [2]. In addition, the selectivity (skirt factor) is optimized from 50% to 92%, and the fractional passband width is raised from 95% to 133% compared with the former UWB BPF in [8].

4. CONCLUSIONS

In this paper, a novel UWB bandpass filter using a back-to-back CPW-microstrip transition structure has been presented and analyzed. Its selectivity is significantly improved due to two transmission zeros located in upper and lower stopbands respectively introduced by a modified T-sharp stub. Finally, to verify the design, a prototype of the proposed filter is fabricated and measured in the frequency band of 1–16 GHz. The proposed filter exhibits good performance both in-band and out-of-band such as sharp selectivity, low insertion loss (< 0.65 dB) with compact size ($0.36\lambda_0 \times 0.17\lambda_0$), which make the proposed filter a good candidate for UWB systems.

ACKNOWLEDGMENT

This work was supported by the National Natural Science Foundation of China (61271034) and the China Postdoctoral Science Foundation (grant No. 2014M552337).

REFERENCES

1. Federal Communications Commission, "Revision of part 15 of the commission's rules regarding ultra-wideband transmission systems," First Report and Order, FCC 02. V48, Apr. 2002.
2. Chu, Q.-X., X.-H. Wu, and X.-K. Tian, "Novel UWB bandpass filter using stub-loaded multiple-mode resonator," *IEEE Microw. Wireless Compon. Lett.*, Vol. 21, No. 8, 403–405, 2011.
3. Deng, H. W., Y. J. Zhao, L. Zhang, X. S. Zhang, and S. P. Gao, "Compact quintuple-mode stub-loaded resonator and UWB filter," *IEEE Microw. Wireless Compon. Lett.*, Vol. 20, No. 8, 438–440, 2010.
4. Taibi, A., M. Trabelsi, A. Slimane, M. T. Belaroussi, and J.-P. Raskin, "A novel design method for compact UWB bandpass filters," *IEEE Microw. Wireless Compon. Lett.*, Vol. 25, No. 1, 4–6, 2015.
5. Chu, Q.-X. and X.-K. Tian, "Design of UWB bandpass filter using stepped-impedance stub-loaded resonator," *IEEE Microw. Wireless Compon. Lett.*, Vol. 20, No. 9, 501–503, 2010.
6. Chen, L.-Y., C.-H. Lee, and C.-I. G. Hsu, "Novel UWB BPF design using modified trisection MMR," *Microw. Opt. Technol. Lett.*, Vol. 50, 2904–2907, 2008.
7. Wang, I.-C., C.-H. Lee, and C.-I. G. Hsu, "Design of band-notched UWB BPF with very wide upper stopband using combined $\lambda/4$ TSSIR," *Journal of Electromagnetic Waves and Applications*, Vol. 23, Nos. 2–3, 183–194, 2009.
8. Hu, H. L., X. D. Huang, and C. H. Cheng, "Ultra-wideband bandpass filter using CPW-to-microstrip coupling structure," *Electron. Lett.*, Vol. 42, No. 10, 586–587, 2006.
9. Wang, K., S. M. Wong, and Q.-X. Chu, "A compact UWB CPW bandpass filter with short-ended H-shaped resonator and controllable notched band," *Microwave. Opt. Technol. Lett.*, Vol. 55, No. 7, 1577–1581, 2013.
10. Xia, X., Y. Liu, H. Lin, T. Yang, and H. Jin, "Novel UWB BPF with a controllable notched band using hybrid structure," *IEICE Electronics Express*, Vol. 14, No. 6, 1–6, 2017.
11. Ghazali, A. N., M. Sazid, and S. Pal, "A miniaturized microstrip-to-CPW transition based UWB-BPF with shaped roll-off and minimum insertion loss," *Microw. Opt. Technol. Lett.*, Vol. 58, No. 2, 289–293, 2016.
12. Ghazali, A. N., M. Sazid, and S. Pal, "Compact broadband balun-based UWB-BPF with minimum insertion loss and sharp selectivity," *Electron. Lett.*, Vol. 51, No. 15, 1174–1175, 2015.
13. Li, J., C. Ding, F. Wei, and X. W. Shi, "Compact UWB BPF with notch band based on SW-HMSIW," *Electron. Lett.*, Vol. 51, No. 17, 1338–1339, 2015.
14. Mirzaee, M., B. S. Virdee, and S. Noghanian, "Compact ultra-wideband bandpass filter with variable notch characteristics based on transversal signal-interaction concepts," *Int. J. RF Microwave Comput-Aid Eng.*, Vol. 24, 549–559, 2014.
15. Feng, W. J., W. Q. Che, and T. F. Eibert, "Ultra-wideband bandpass filter based on transversal signal-interaction concepts," *Electron Lett.*, Vol. 24, 1330–1331, 2011.
16. Fallahzadeh, S. and M. Tayarani, "A new microstrip UWB bandpass filter using defected microstrip structures," *Journal of Electromagnetic Waves and Applications*, Vol. 24, No. 7, 893–902, 2010.
17. Lin, H., H. Peng, X. Xia, T. Yang, and H. Jin, "A novel ultra-wideband bandpass filter using defected microstrip structures," *IEICE Electron. Expr.*, Vol. 13, No. 7, 1–6, 2016.
18. Tang, I.-T., D.-B. Lin, C.-M. Li, and M.-Y. Chiu, "Compact pentagon ultra-wideband bandpass filter with good out-of-band performance," *Journal of Electromagnetic Waves and Applications*, Vol. 23, No. 13, 1695–1706, 2009.